Clinical Cases in Medicine

ISSN: 2770-2359

Research Article

Identification of Novel *PRKAG3* Isoform in Indian Glioma Patient Samples

Megha Chaudhary[1#], Gargi Nandi[1#], Naveen Soni[1], Nargis[3], Sushmita Jha[2], Kunzang Chosdol[3], Rajdeep Chowdhury[4] and Bhawana Bissa[1]*

[1]*Department of Biochemistry, Central University of Rajasthan, India*

[2]*Department of Biosciences and Bioengineering, Indian Institute of Technology, India*

[3]*Department of Biochemistry, All India Institute of Medical Sciences, India*

[4]*Department of Biological Sciences, Birla Institute of Technology and Science (BITS), India*

[#]*These authors contributed equally*

Abstract

Aim: Alternative splicing in cancer can be attributed to several factors. Cancer cells undergo extensive molecular and genetic changes, leading to dysregulation of splicing machinery and aberrant splicing patterns. It's important to note that the exact mechanisms driving increased alternative splicing in cancer are still being actively researched, and the landscape of splicing changes can vary across different cancer types. Cancer cells also look for various mechanisms to survive better in stress, which can be either by dysregulation of splicing factors, genome alterations, or epigenetic modifications. The increased protein repertoire in cancer cells can contribute to various aspects of tumorigenesis, including altered signaling pathways, enhanced cell survival, increased angiogenesis, and evasion of immune surveillance.

Methods: We worked on a total of 30 GBM patient samples and 15 LGG patient samples, along with the normal brain, and glioblastoma cell lines, and we checked the expression level of *PRKAG3*. We have also done the in-silico analysis of the same in different databases such as TCGA, HPA, and CCGA. Then we identified the novel isoform of *PRKAG3* by performing polymerase chain reaction.

Results: Here, we have reported the expression of *PRKAG3* and its isoforms in GBM and Low-Grade Glioma (LGG) might be exclusive in the Asian population as we didn't find databases like The Cancer Genome Atlas (TCGA) and Human Protein Atlas (HPA). Apart from this, we found out that the expression of *PRKAG3* is dependent on the stage of the brain tumor. We have also shown that expression of *PRKAG3* can be an indicator of poor prognosis of glioblastoma concerning Isocitrate Dehydrogenase (*IDH*) mutations as well, which is one of the important enzymes involved in various cellular pathways.

Conclusion: The study presents significant association of higher expression of novel splice variant of *PRKAG3* in low grade glioma and reduced expression in glioblastoma multiforme. This study might be of significant value in future discovery of biomarkers and prognosis marker for glioma progression.

Introduction

Alternative splicing is a cellular process wherein one gene can generate different types of mRNA transcripts, simply by joining exons in varied combinations [1]. The phenomenon is fairly common in humans, where about 94% of human genes have intronic regions in the pre-mRNA steps. It is also well established that most eukaryotic genes undergo temporal and spatial splicing events that are regulated by RNA Binding Proteins (RBPs), cis-acting and trans-acting elements [2]. Alternative splicing is not a rare phenomenon when we deal with cancer cells. Splicing abnormalities are often observed to be associated with tumor progression. Many splicing factors are mis-regulated in cancer cells. Changes in the expression levels or activities of splicing factors can lead to altered splicing patterns. Dysfunctional splicing factors can result in the inclusion or exclusion of specific exons, leading to the production of aberrant protein isoforms with distinctively different functions. Therefore, alternative splicing is a key event of cells' response to stimuli and thus, is linked to cancer progression in response to the tumor microenvironment [3]. There are some examples of alternative splicing events that have been implicated in cancer. For example, CD44 [4] is a cell surface glycoprotein involved in cell adhesion, migration, and signaling [5,6]. Alternative splicing of CD44 generates various isoforms, including the standard isoform (CD44s) and variant isoforms (CD44v). CD44v isoforms have in turn been associated with tumor progression, metastasis, and poor prognosis in multiple cancer types, including colorectal cancer [7,8]. Similarly, Bcl-x is a member of the Bcl-2 [9] family of proteins involved in the regulation of apoptosis (programmed cell death) [10,11]. Alternative splicing of Bcl-x produces two main isoforms: Bcl-xL, which inhibits apoptosis, and Bcl-xS, which promotes apoptosis. Dysregulation of Bcl-x splicing has been observed in several cancer types, including breast, lung, and prostate cancer, and it can confer resistance to apoptosis and promote tumor survival [12,13]. In addition, VEGF [14] is a key regulator of angiogenesis, the formation of new blood vessels [15,16]. Alternative splicing of VEGF pre-mRNA generates multiple isoforms, including VEGF-Axxx (pro-angiogenic) and VEGF-Axxxb (anti-angiogenic). Dysregulation of VEGF alternative splicing has been reported in several cancer types, including breast, ovarian, and colorectal cancer, and it can promote tumor angiogenesis and metastasis [17].

On a similar note, AMPK is a highly conserved serine/threonine protein kinase that acts as a critical regulator of cellular energy homeostasis [18]. The AMPK complex consists of three subunits: a

Citation: Chaudhary M, Nandi G, Soni N, Nargis, Jha S, Chosdol K, et al. Identification of Novel *PRKAG3* Isoform in Indian Glioma Patient Samples. Clin Cases Med. 2024;4(1):1022.

Publisher Name: Medtext Publications LLC

Manuscript compiled: Jan 06th, 2024

***Corresponding author:** Bhawana Bissa, Department of Biochemistry, Central University of Rajasthan, Ajmer, Rajasthan 305817, India

catalytic α subunit, a regulatory β subunit, and a regulatory γ subunit, with multiple isoforms for each subunit [19]. Herein, the *PRKAG3* [20] gene specifically encodes the γ3 isoform of the regulatory subunit, [21] and it serves as the regulatory subunit that senses the AMP-to-ATP ratio within the cell and allosterically activates AMPK in response to energy stress. *PRKAG3* is primarily expressed in skeletal muscle tissue, where it plays a critical role in regulating energy metabolism. Activation of AMPK through *PRKAG3* promotes ATP production and stimulates glucose uptake, fatty acid oxidation, and mitochondrial biogenesis in skeletal muscle cells [22]. *PRKAG3* is involved in the regulation of glycogen synthesis and storage in skeletal muscle. Mutations in *PRKAG3* have been associated with glycogen storage disease type 10 (GSD10), characterized by abnormal glycogen accumulation in skeletal muscle fibers [23]. *PRKAG3* has no reported expression in brain and brain tumors. While working with AMPK subunit expression in Glioblastoma Multiforme (GBM) and low-Grade Glioma (LGG), we came across patient samples that showed expression of *PRKAG3*. This paper reports the expression of *PRKAG3* and its isoforms in GBM and LGG in the Asian population.

Methods

Sample acquisition

All patient samples were acquired as RNA samples in the lab of Dr. Kunzang Chosdol at All India Institute of Medical Sciences (AIIMS), Delhi, India for which the ethical clearance has been obtained from AIIMS Ethics committee. They were well labeled and stored at -800°C. The samples were transported to the laboratory in a sealed box filled with dry ice and again stored at -800°C till further use. Normal brain total RNA was purchased from Clontech (catalog no. 636530)

PCR

Polymerase Chain Reaction (PCR) is a commonly used molecular biology technique that allows for the amplification of specific DNA sequences. It is a versatile tool that enables researchers to generate millions of copies of a target DNA region, even from a tiny amount of starting material. PCR has revolutionized various fields of research, including genetics, forensics, diagnostics, and biotechnology. We used Takara 2X master mix, along with primer pair, cDNA as template, and nuclease-free water to make a 10 µl PCR reaction. The PCR products were run in 1% agarose-EtBr gel at 90V for 45 minutes. The images were then visualized using a gel documentation system.

RT-PCR

Real-time Polymerase Chain Reaction (PCR), also known as quantitative PCR (qPCR), is a widely used molecular biology technique that allows for the detection and quantification of specific DNA or RNA molecules in real-time. It is a more advanced and refined version of conventional PCR. Real-time PCR incorporates the use of fluorescent dyes or probes to monitor the amplification of the target DNA or RNA during the PCR reaction. The technique relies on the principle of DNA amplification through multiple cycles of heating and cooling, using specific primers that bind to the target sequence of interest. We used SYBR green as the fluorescent dye for real-time PCR and set up each reaction in triplicates. We then analyzed the fold changes through MS Excel and plotted graphs using GraphPad Prism software.

Gel purification

Nucleic acid gel purification is a commonly used technique in molecular biology that allows for the isolation and purification of specific DNA or RNA fragments from an agarose gel matrix. This technique is often performed following gel electrophoresis, where DNA or RNA molecules are separated based on their size through an electric field. Gel purification enables the isolation of target fragments for downstream applications such as cloning, sequencing, PCR, or other molecular analyses. We used the GCC Biotech® Gsure gel extraction kit to purify the PCR products from agarose gel pieces.

DNA sequencing

DNA sequencing using Illumina technology is a high-throughput sequencing method that enables rapid and cost-effective analysis of DNA sequences. Illumina sequencing, also known as Next-Generation Sequencing (NGS), has revolutionized genomics research and has numerous applications in fields such as medicine, agriculture, and environmental studies. Illumina sequencing technology offers several advantages, including high throughput, scalability, and cost-effectiveness. It has enabled the sequencing of whole genomes, targeted sequencing of specific regions, transcriptome analysis, metagenomics studies, and many other applications. The data generated through Illumina sequencing has significantly contributed to our understanding of genetics, disease research, and personalized medicine.

TCGA, CGGA, and HPA

The Cancer Genome Atlas (TCGA) is a groundbreaking initiative launched by the National Cancer Institute (NCI) and the National Human Genome Research Institute (NHGRI) in the United States. TCGA aimed to comprehensively characterize genomic alterations in various cancer types, providing researchers with a wealth of molecular data to better understand the underlying mechanisms of cancer development and progression. TCGA utilizes high- throughput sequencing technologies to generate genomic, transcriptomic, and epigenomic data from thousands of tumor samples across multiple cancer types. The project also collected corresponding clinical data, facilitating the correlation of molecular alterations with patient outcomes.

The Chinese Glioma Genome Atlas (CGGA) is a large-scale research project focused on glioma, a type of brain tumor. It aims to uncover the genetic and molecular characteristics of gliomas in the Chinese population, providing valuable insights into tumor biology and potential therapeutic targets. CGGA collects clinical information, genomic data, and other relevant molecular information from glioma patients in China. It utilizes advanced genomic sequencing technologies to analyze the DNA, RNA, and epigenetic profiles of tumor samples, enabling researchers to identify genetic alterations and molecular subtypes associated with glioma development and progression.

The Human Protein Atlas (HPA) is a comprehensive resource that provides information on the expression, localization, and function of human proteins in various tissues and cells. It is a collaborative effort involving researchers from Sweden and other international partners. The HPA utilizes Immunohistochemistry (IHC), Immunofluorescence (IF), and other advanced techniques to systematically map the expression patterns of proteins across different human tissues and cell lines. The project aims to create a detailed protein atlas that can serve as a valuable reference for researchers studying protein function and disease mechanisms.

Statistical analysis

Data are presented as the mean ± Standard Error of the Mean

(SEM). Data were analyzed using GraphPad Prism 7.02 software (GraphPad Software Inc., CA, USA). Statistical significance was determined using Student's t test.

Results

Expression analysis of AMPK subunits in GBM cell lines, normal brain, GBM, and LGG patient samples

Expression analysis was done by performing Polymerase Chain Reaction (PCR) using the cDNA of GBM cell lines, U87MG and LN229, normal brain, and GBM and LGG patient samples, along with gene-specific primers. Primer pairs were designed for all the AMPK genes using primer BLAST [24] and Primer3 [25] tools. The primers designed had an annealing temperature of 600, except for *PRKAG3*, for which the primer pair had an annealing temperature of 580 (Figure 1B). The amplicon sizes were all in the range of 100 bp-200 bp (Figure 1B). A PCR reaction for 18S rRNA was set as a positive control as well as a size estimate as the amplicon of 18S rRNA is of 99bp. The gel images were then compared to check the expression of the AMPK genes (Figure 1A). Interestingly, an amplicon of *PRKAG3* was observed only in GBM and LGG patient samples. Moreover, the amplicon was seen of a higher size (445 bp) than the expected size of 117 bp. Therefore, we suspected intron retention as the possible reason for higher size of *PRKAG3* amplicon

In-silico analysis of *PRKAG3* expression across TCGA, HPA, and CCGA datasets

On finding the amplicon of *PRKAG3* in patient samples, we tried to look in the existing databases for any similar pattern of expression. The Cancer Genome Atlas (TCGA) datasets were accessed using the bioinformatic tool, GEPIA2 [26] where we checked for the expression of *PRKAG3* across all cancer types. The bar graph so obtained (Figure 2A) was the log TPM (Transcripts per Million) values of *PRKAG3* in normal and tumor tissues of 31 cancers. It was seen that *PRKAG3* was mostly expressed in normal samples, the highest expression being in Head and Neck Squamous Cell Carcinoma (HNSC), followed by Tenosynovial Giant Cell Tumors (TGCT), Skin Cutaneous Melanoma (SKCM), and Prostate Adenocarcinoma (PRAD), and a comparatively lower expression was observed in Urothelial Bladder Carcinoma (BLCA), Breast Invasive Carcinoma (BRCA), Esophageal Carcinoma (ESCA), Lung Adenocarcinoma (LUAD), Lung Squamous Cell Carcinoma (LUSC), and Sarcoma (SARC). On the other hand, *PRKAG3* was slightly expressed in tumors of HNSC, Uterine Carcinosarcoma (UCS), ESCA, LUSC, Ovarian Serous Cystadenocarcinoma (OV), SARC, Thymoma (THYM), PRAD, and SKCM. OV and THYM were the only cancer types wherein the expression of *PRKAG3* was observed when their normal tissue counterparts did not have expression. The key point to note in the data was that GBM and LGG had no expression of *PRKAG3* in both normal and tumor types. This went well with our PCR results of normal brain and the GBM cell lines, LN229 and U87MG. However, we did not find any synchrony with the expression of *PRKAG3* we observed in the patient samples. Also, there was no expression of *PRKAG3* when checked on Human Protein Atlas (HPA) except for a high expression in skeletal muscles (Supplementary Figure 1A and 1B).

Next, we moved on to analyze mRNA data from the Chinese Glioma Genome Atlas (CGGA). CGGA had 3 mRNA datasets: mRNAseq_325 [27-30], mRNAseq_693, [27,31-33] and, mRNA_array_301 [27,34,35]. Out of these 3 datasets, mRNA_array_301 had the expression of *PRKAG3* in Glioma samples. The dataset was presented in the form of boxplots of *PRKAG3* expression in different patient categories. The data were categorized into histology of the tumor, WHO grade, *IDH* mutation status, 1p/19q deletion status, gender, and age. The significance of the gene expression was checked using ANOVA and t-test. There was significant expression of *PRKAG3* when the data were categorized based on histology, WHO grade, *IDH* mutation status, and 1p/19q co-deletion status (Supplementary Figure 2A-D). However, the expression of *PRKAG3* was not significant when the data were categorized based on age and gender (Supplementary Figure 2E and F).

Identification of novel isoforms of *PRKAG3* in GBM and LGG samples

We performed PCR on all the GBM and LGG patient samples for the *PRKAG3* gene. First, all 19 male GBM patient cDNAs were arranged in increasing order of age, and PCR reactions were set using *PRKAG3* primers. 18S rRNA was used as a positive control for all cDNA. Nine of the male samples showed varied degrees of amplification of *PRKAG3* alternative splice variant (Figure 3A). The amplification was random and not based on the age of the patients. Similarly, *PRKAG3* amplification was checked in 11 female GBM patient samples. Six female samples displayed amplification of higher amplicon of *PRKAG3* (Figure 3B). We further conducted Real-time PCR for 2 male samples and 2 female samples which had a good amplification of *PRKAG3*. Sample no. 11 and sample no. 91 were the male samples and sample no. 28 and sample no. 92 were the female samples for which Real-time PCR was done. 18s rRNA was set as a positive PCR control and normal brain cDNA was also set up as control for comparison of *PRKAG3* expression as done for the PCR reactions of male and female GBM patients. We then plotted the fold change of *PRKAG3* expression of the normal brain, 2 male and 2 female patient samples (Figure 3C) Sample no. 11 had about 300 times the relative gene expression of *PRKAG3*. Sample no. 91 and sample no. 92 displayed about 50 times the relative expression of *PRKAG3*. Lastly, sample no. 28 had about 8 times the relative gene expression of *PRKAG3*.

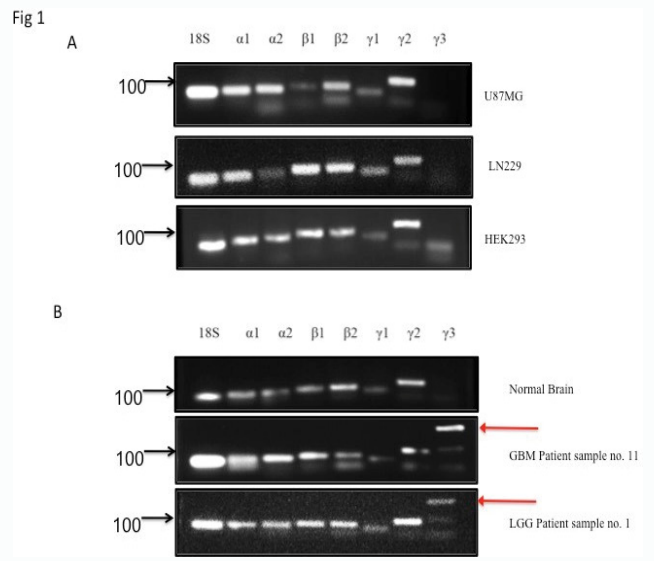

Figure 1: Expression analysis of AMPK subunits in GBM cell lines, normal brain, GBM and LGG patient samples. A) PCR amplicons of all *AMPK* genes (*PRKAA1*, *PRKKA2*, *PRKAB1*, *PRKAB2*, *PRKAG1*, *PRKAG2* and *PRKAG3*) along with housekeeping gene 18S rRNA in *U87MG*, *LN229* and *HEK293* cell lines. B) PCR amplicons of all AMPK genes (*PRKAA1*, *PRKKA2*, *PRKAB1*, *PRKAB2*, *PRKAG1*, *PRKAG2* and *PRKAG3*) along with housekeeping gene 18S rRNA in Normal Brain, GBM patient sample no.11 and LGG patient sample no. 1.

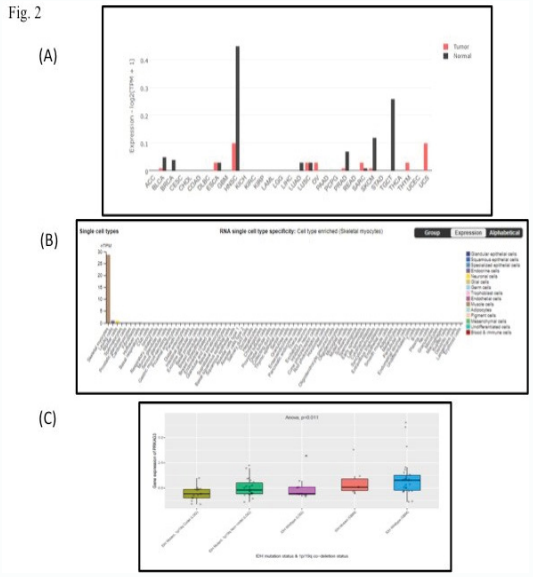

Figure 2: In-silico analysis of *PRKAG3* expression across TCGA, HPA, and CCGA datasets. A) Bar Graph generated through GEPIA2 showing Expression of *PRKAG3* in log TPM scale in all cancer types on the basis of TCGA datasets. B) Bar Graph generated using Human Protein Atlas showing RNA level of *PRKAG3* in various cells of the body. C) Box plot of mRNA_array_301 dataset in CGGA showing expression of *PRKAG3* on the basis of IDH mutation status & 1p/19q co−deletion status.

Similarly, PCR reactions of 15 LGG samples were also set up. The samples were not arranged according to age but were arranged according to serial numbers. All the samples showed high expression of higher splice variant of *PRKAG3* (Supplementary Figure 3A). We then did spot densitometry of the amplified bands and then plotted a graph of mean gray values of the bands (Supplementary Figure 3B) LGG samples showed significantly high expression of novel splice variant as compared to GBM samples.

Scanning of other exon junctions of one GBM patient cDNA

We designed primers that encompassed other exon junctions of the *PRKAG3* gene. We retrieved all the sequence information of the gene from NCBI. The gene has 13 exons and the previously designed primer sets covered exon 6 and exon 8 partially (Figure 4A). This being said, exon 7 was completely covered in the amplicon. 2 introns, intron 6 and intron 7, were also therefore within the range of the primers. Thus, a total of 4 exon-intron junctions were covered in the previously designed primers and the amplicon size increased to 445 bp, both the covered introns were included (Figure 4B). Since the theoretical amplicon size was close to the amplicon size, we were observing in the gel images, this was our first confirmation of intron retention in *PRKAG3*.

We then designed 4 sets of primers covering different regions of *PRKAG3*. The coding sequence of *PRKAG3*, having just the exons, was retrieved from Ensembl and was used as a template for designing primers (Figure 4C). We tried to cover as many exon-exon junctions as possible. The first set of primers, *PRKAG3*-I, covered the exon junction between the first exon and the second exon as well as the junction between the second exon and the third exon. The second set of primers, *PRKAG3*-II, was designed within the fourth exon. The third set of primers, *PRKAG3*-III, covered the junction between the eighth and ninth exon. The last pair of primers, *PRKAG3*-IV, covered from the tenth to the thirteenth exon (Supplementary Figure 4A). All the primers were designed using primer BLAST and Primer3 tools.

We amplified the GBM patient sample no. 7 cDNA using these primers. While the first and the fourth set of primers displayed smearing in their gel lanes, the second and the third set of primers, *PRKAG3*-II and *PRKAG3*-III, showed crisp amplicon bands on the agarose gel (Supplementary Figure 4B) *PRKAG3*-II primers were designed within an exon so the amplicon was obtained at the expected size. But, *PRKAG3*-III primers gave a larger amplicon suggesting that the ninth intron might also be retained in GBM patient sample no. 7.

Intron retention revealed from sequencing of novel isoforms

We amplified GBM patient sample no. 11 cDNA with the initial set of primers and GBM patient sample no. 7 cDNA with *PRKAG3*-III primers. These patient samples were selected as they had good amplification of *PRKAG3*. We visualized the bands in UV light and cut the amplified bands from the gel matrix using a sterile blade. We then extracted the PCR products from the gel using the GCC biotech® Gsure gel extraction kit. The protocol was used as per the instructions provided with the kit. 10 µl of the eluted product was sent for sequencing along with primers used for amplification. The quality control gel image showed the amplicon of patient no. 7 at about 300 bp and the amplicon of patient no. 11 at about 400 bp. (Figure 5C).

Upon sequencing, the electropherograms obtained were scale adjusted using the Finch TV software. The sequences obtained were subjected to BLAST analysis against the complete sequence of *PRKAG3*. The PCR product obtained from patient no. 11 was 99% identical with the 3771-4144 bp region of *PRKAG3* (Figure 5A and B) This region falls in the intron-retained version of the gene that we analyzed previously (Figure 4A) The DNA sequencing, therefore, reinstates that intron 7 and intron 8 of *PRKAG3* are retained.

Similarly, The PCR product obtained from patient no. 7 was 99% identical with the 4178 bp-4450 bp region of *PRKAG3* (Supplementary Figure 5A and B) In this case, intron 9 is being retained and thus we obtained a larger amplicon size of 339 bp as opposed to 138 bp if the intron had not been retained (Supplementary Figure 5C).

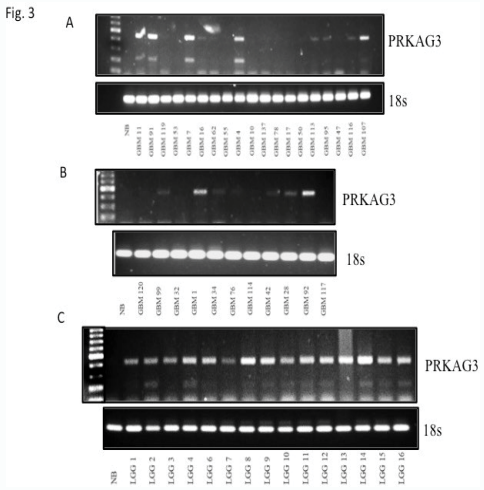

Figure 3: Identification of novel isoforms of *PRKAG3* in GBM and LGG samples. A) PCR amplicons of *PRKAG3* and 18S rRNA in all male GBM patient samples. B) PCR amplicons of *PRKAG3* and 18S rRNA in all female GBM patient samples. C) PCR amplicons of *PRKAG3* and 18S rRNA in all LGG patient samples.

Fig 4

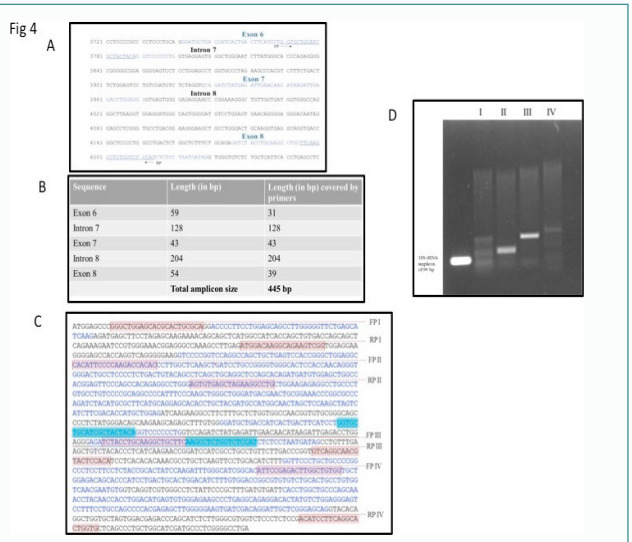

Sequence	Length (in bp)	Length (in bp) covered by primers
Exon 6	59	31
Intron 7	128	128
Exon 7	43	43
Intron 8	204	204
Exon 8	54	39
	Total amplicon size	445 bp

Figure 4: Scanning of other exon junctions of one GBM patient cDNA. A) Picture of showing a portion of PRKAG3 gene sequence (3721-4260 bp) indicating primer position and the introns and exons involved. B) Table depicting the introns and exons covered in the increased amplicon size of *PRKAG3*. C) Picture showing all exons of *PRKAG3* in alternating colours with previous *PRKAG3* primers highlighted in cyan and newly designed *PRKAG3* highlighted in faint red.

Fig 5

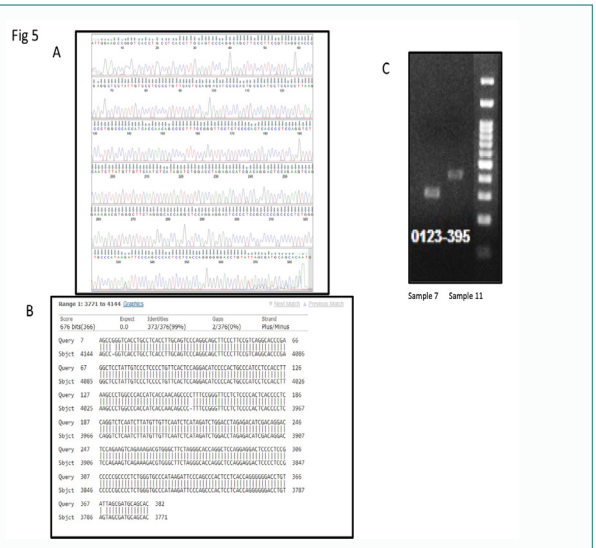

Figure 5: Intron retention revealed from sequencing of novel isoforms. A) Sequencing results in the form of electropherograms for PCR product obtained by amplifying GBM patient sample no. 11 using the previous primers. B) BLAST of obtained sequence of sample 11 amplicon against the CDS of *PRKAG3*. C) QC gel image sent by the sequencing company depicting the quality of gel purified PCR products that were sent.

Thus, through sequencing, it was confirmed that *PRKAG3* is being transcribed in GBM samples and showing different splice variants.

Discussion

We worked on a total of 30 GBM patient samples and 15 LGG patient samples, along with the normal brain, U87MG, LN229, and HEK293T cell lines. The expression of *PRKAG3* was seen in the PCR reactions done using the cDNA prepared from patient samples, whereas the expression was not seen in any of the brain tumor cell lines and HEK293T cell lines. We further validated our results by conducting RT-PCR of selected GBM patients and saw significant fold changes in *PRKAG3* as compared to the normal brain. Not only the expression of the gene was observed, but the intron retention and splice variants were discovered in GBM patients. This was confirmed through sequencing and BLAST analysis of PCR products. Moreover, we checked databases to find *PRKAG3* expression in the brain and brain tumors. We found some similar data in Chinese Glioma Genome Atlas (CGGA) database regarding the expression of *PRKAG3* in GBM, but no data regarding *PRKAG3* expression was seen in databases like The Cancer Genome Atlas (TCGA) and Human Protein Atlas (HPA). Hence, we concluded that the expression of *PRKAG3* in brain tumors might be exclusive to the Asian population. The expression of *PRKAG3* was not affected by age or gender. Rather, we saw the expression of *PRKAG3* in all LGG samples but only 50 percent of the GBM samples had the expression of *PRKAG3*. Therefore, we believe that the expression of *PRKAG3* is dependent on the stage of the brain tumor. Our presumption is also backed by the data obtained from CGGA, where there was a significant expression of *PRKAG3* based on histology, WHO grade, *IDH* mutation status, and 1p/19q co-deletion status. In the CGGA data, based on histology, the highest expression of *PRKAG3* was in GBM, followed by recurrent Anaplastic Astrocytoma (rAA), and recurrent Astrocytoma (rA). Next, rGBM, astrocytoma (A), and Anaplastic Oligodendroglioma (AO) had almost equal expression. Finally, Anaplastic Astrocytoma (AA) and oligodendroglioma (O) had the least expression of *PRKAG3*. Based on the WHO grade, grade IV had the highest expression followed by grade II, and the least in grade III. Based on *IDH* mutation status, the wild type had more expression of *PRKAG3* than the mutant type. Lastly, based on the 1p/19q co- deletion status, non-co-deleted samples had higher *PRKAG3* expression than the co-deleted samples. 1p/19q Co-deletion in gliomas is a rare event [36,37]. It comprises a complete deletion of the short arm of chromosome 1 and the long arm of chromosome 19 together. Glioma patients with this co-deletion are known to show better prognosis and survival than those without this co-deletion [38-40]. Since the non-codeletion had more expression of *PRKAG3*, it can be hypothesized that *PRKAG3* expression can lead to a poor prognosis. Isocitrate Dehydrogenase (*IDH*) [41,42] enzymes are vital enzymes involved in several crucial metabolic processes. There are three isoforms of *IDH*, each playing essential roles in various cellular pathways. These enzymes are integral to the functioning of the Krebs cycle, glutamine metabolism, lipogenesis, and redox regulation, among other important metabolic processes [43-45]. Mutations in the *IDH* gene are commonly observed in various types of cancer. *IDH* mutations are highly prevalent in gliomas, being present in more than 80% of cases classified as World Health Organization (WHO) grade II/III [46]. These mutations are also frequently observed in secondary glioblastomas, accounting for 73% of clinical cases. However, primary glioblastomas show a lower occurrence of *IDH* mutations, being detected in only 3.7% of cases [47]. *IDH* mutations are associated with a more favorable prognosis and extended median survival in certain types of brain tumors. In Glioblastoma (GBM), patients with *IDH* mutations have a prolonged median survival of 31 months compared to 15 months in those with wild-type *IDH*. Similarly, in anaplastic astrocytoma, individuals with *IDH* mutations experience a significantly longer median survival of 65 months compared to 20 months for those with wild-type *IDH* [46]. While gliomas with *IDH* mutations typically demonstrate a more favorable disease outcome, the prevalence of *IDH* mutations in recurrent GBM suggests that lower-grade gliomas with *IDH* mutations often experience recurrence due to malignant transformation into a higher-grade tumor [48]. Furthermore, *IDH*-mutated gliomas are more prone to developing a hypermutation phenotype, which is associated with a poorer prognosis

[49]. Together with the pre-existing knowledge about the association of gliomas with *IDH* mutations, our findings about *PRKAG3* expression can be used in prognostic studies in gliomas. This is because there was a significantly high expression of *PRKAG3* in the wild- type *IDH* data. Again, like in the case of 1p/19q Co-deletion, expression of *PRKAG3* can be an indicator of poor prognosis concerning *IDH* mutations as well. While there have been splice variants of LKB1 (Liver kinase B1; upstream activating kinase for the AMPK [50]) reported, and splice variants of PRKAG2 (protein kinase AMP-activated non-catalytic subunit γ2), as known in previous research, neither the splice variants of *PRKAG3* have been reported previously nor their expression in brain tumors. Our findings, thus report both a new splice variant of *PRKAG3* as well as its novel expression in brain tumors.

Declarations

Ethics approval

Ethics approval was obtained from AIIMS, New Delhi

Competing interests

The authors have no relevant financial or non-financial interests to disclose.

Funding

This work was supported by DST-SERB start-up research grant (SRG/2020/000392) and ICMR extra mural research grant (52/27/2020-BIO/BMS) to Dr. Bhawana Bissa.

Authors' contributions

All authors contributed to the study conception and design. Gargi Nandi, Megha Choudhury, Naveen Soni: Conceptualization, writing, Figure preparation; Nargis, Kunzang Chosdol: Sample collection and ethical clearance; Dr. Rajdeep Chowdhury, Dr. Sushmita Jha: Writing and proof reading; Bhawana Bissa: Conceptualization, writing, supervision. All authors read and approved the final manuscript.

Acknowledgements

Department of Biochemistry, Central University of Rajasthan, India for providing research facility. DST-SERB and ICMR for providing funding. AIIMS, Delhi for providing ethical clearance for sample collection.

References

1. Alternative Splicing. NHGRI. 2024.
2. Pan Q, Shai O, Lee LJ, Frey BJ, Blencowe BJ. Deep surveying of alternative splicing complexity in the human transcriptome by high-throughput sequencing. Nat Genet. 2008;40(12):1413-5.
3. Biamonti G, Catillo M, Pignataro D, Montecucco A, Ghigna C. The alternative splicing side of cancer. Semin Cell Dev Biol. 2014;32:30-6.
4. Senbanjo LT, Chellaiah MA. CD44: A Multifunctional Cell Surface Adhesion Receptor Is a Regulator of Progression and Metastasis of Cancer Cells. Front Cell Dev Biol. 2017;5:18.
5. Orian-Rousseau V. CD44, a therapeutic target for metastasizing tumors. Eur J Cancer. 2010;46(7):1271-7.
6. Ponta H, Sherman L, Herrlich PA. CD44: From adhesion molecules to signaling regulators. Nat Rev Mol Cell Biol. 2003;4(1):33-45.
7. Zeilstra J, Joosten SPJ, Dokter M, Verwiel E, Spaargaren M, Pals ST. Deletion of the WNT target and cancer stem cell marker CD44 in Apc(Min/+) mice attenuates intestinal tumorigenesis. Cancer Res. 2008;68(10):3655-61.
8. Toole BP. Hyaluronan-CD44 Interactions in Cancer: Paradoxes and Possibilities. Clin Cancer Res. 2009;15(24):7462-8.
9. Warren CFA, Wong-Brown MW, Bowden NA. BCL-2 family isoforms in apoptosis and cancer. Cell Death Dis. 2019;10(3):177.
10. Boise LH, González-García M, Postema CE, Ding L, Lindsten T, Turka LA, et al. bcl-x, a bcl-2-related gene that functions as a dominant regulator of apoptotic cell death. Cell. 1993;74(4):597-608.
11. Minn AJ, Vélez P, Schendel SL, Liang H, Muchmore SW, Fesik SW, et al. Bcl-x(L) forms an ion channel in synthetic lipid membranes. Nature. 1997;385(6614):353-7.
12. Schlange T, Matsuda Y, Lienhard S, Huber A, Hynes NE. Autocrine WNT signaling contributes to breast cancer cell proliferation via the canonical WNT pathway and EGFR transactivation. Breast Cancer Res. 2007;9(5):R63.
13. Tu Y, Renner S, Xu F, Fleishman A, Taylor J, Weisz J, et al. BCL-X expression in multiple myeloma: a possible indicator of chemoresistance. Cancer Res. 1998;58(2):256-62.
14. Shibuya M. Vascular Endothelial Growth Factor (VEGF) and Its Receptor (VEGFR) Signaling in Angiogenesis: A Crucial Target for Anti- and Pro-Angiogenic Therapies. Genes Cancer. 2011;2:1097-105.
15. Carmeliet P, Ferreira V, Breier G, Pollefeyt S, Kieckens L, Gertsenstein M, et al. Abnormal blood vessel development and lethality in embryos lacking a single VEGF allele. Nature. 1996;380(6573):435-9.
16. Ferrara N, Gerber HP, LeCouter J. The biology of VEGF and its receptors. Nat Med. 2003;9(6):669-76.
17. Matteo AD, Belloni E, Pradella D, Cappelletto A, Volf N, Zacchigna S, et al. Alternative splicing in endothelial cells: novel therapeutic opportunities in cancer angiogenesis. J Exp Clin Cancer Res. 2020;39(1):275.
18. Herzig S, Shaw RJ. AMPK: Guardian of metabolism and mitochondrial homeostasis. Nature Reviews Molecular Cell Biology. 2018;19:121-35.
19. Ross FA, MacKintosh C, Hardie DG. AMP-activated protein kinase: a cellular energy sensor that comes in 12 flavors. FEBS J. 2016;283(16):2987-3001.
20. PRKAG3 protein kinase AMP-activated non-catalytic subunit gamma 3 [Homo sapiens (human)].
21. PRKAG3 protein kinase AMP-activated non-catalytic subunit gamma 3 [Homo sapiens (human)].
22. Jørgensen SB, Viollet B, Andreelli F, Frøsig C, Birk JB, Schjerling P, et al. Knockout of the alpha2 but not alpha1 5'-AMP-activated protein kinase isoform abolishes 5-aminoimidazole-4-carboxamide-1-beta-4-ribofuranosidebut not contraction-induced glucose uptake in skeletal muscle. J Biol Chem. 2004;279(2):1070-9.
23. Burwinkel B, Hu B, Schroers A, Clemens PR, Moses SW, Shin YS, et al. Muscle glycogenosis with low phosphorylase kinase activity: mutations in PHKA1, PHKG1, or six other candidate genes explain only a minority of cases. Eur J Hum Genet. 2003;11:516-26.
24. Altschul SF, Gish W, Miller W, Myers EW, Lipman DJ. Basic local alignment search tool. J Mol Biol. 1990;215(3):403-10.
25. Untergasser A, Cutcutache I, Koressaar T, Ye J, Faircloth BC, Remm M, et al. Primer3--new capabilities and interfaces. Nucleic Acids Res. 2012;40(15):e115.
26. Tang Z, Kang B, Li C, Chen T, Zhang Z. GEPIA2: an enhanced web server for large- scale expression profiling and interactive analysis. Nucleic Acids Res. 2019;47(W1):W556-60.
27. Zhao Z, Zhang KN, Wang Q, Li G, Zeng F, Zhang Y, et al. Chinese Glioma Genome Atlas (CGGA): A Comprehensive Resource with Functional Genomic Data from Chinese Glioma Patients. Genomics Proteomics Bioinformatics. 2021;19(1):1-12.
28. Zhang K, Liu X, Li G, Chang X, Li S, Chen J, et al. Clinical management and survival outcomes of patients with different molecular subtypes of diffuse gliomas in China (2011-2017): a multicenter retrospective study from CGGA. Cancer Biol Med. 2022;19(10):1460-76.
29. Wang Y, Qian T, You G, Peng X, Chen C, You Y, et al. Localizing seizure-susceptible brain regions associated with low-grade gliomas using voxel-based lesion-symptom mapping. Neuro Oncol. 2015;17(2):282-8.
30. Liu X, Li Y, Qian Z, Sun Z, Xu K, Wang K, et al. A radiomic signature as a non-

invasive predictor of progression-free survival in patients with lower-grade gliomas. Neuroimage Clin. 2018;20:1070-7.

31. Zhao Z, Meng F, Wang W, Wang Z, Zhang C, Jiang T. Comprehensive RNA-seq transcriptomic profiling in the malignant progression of gliomas. Sci Data. 2017;4:170024.

32. Bao ZS, Chen HM, Yang MY, Zhang CB, Yu K, Ye WL, et al. RNA-seq of 272 gliomas revealed a novel, recurrent PTPRZ1-MET fusion transcript in secondary glioblastomas. Genome Res. 2014;24(11):1765-73.

33. Fang S, Liang J, Qian T, Wang Y, Liu X, Fan X, et al. Anatomic Location of Tumor Predicts the Accuracy of Motor Function Localization in Diffuse Lower-Grade Gliomas Involving the Hand Knob Area. AJNR Am J Neuroradiol. 2017;38(10):1990-97.

34. Wang Y, Wang Y, Fan X, Li S, Liu X, Wang J, et al. Putamen involvement and survival outcomes in patients with insular low- grade gliomas. J Neurosurg. 2017;126(6):1788-94.

35. Fuller CE, Perry A. Molecular Diagnostics in Central Nervous System Tumors. Adv Anat Pathol. 2007;12(4):180-94.

36. Eckel-Passow JE, Lachance DH, Molinaro AM, Walsh KM, Decker PA, Sicotte H, et al. Glioma Groups Based on 1p/19q, IDH, and TERT Promoter Mutations in Tumors. N Engl J Med. 2015;372(26):2499-508.

37. van den Bent MJ, Brandes AA, Taphoorn MJB, Kros JM, Kouwenhoven MCM, Delattre JY, et al. Adjuvant Procarbazine, Lomustine, and Vincristine Chemotherapy in Newly Diagnosed Anaplastic Oligodendroglioma: Long-Term Follow-Up of EORTC Brain Tumor Group Study 26951. J Clin Oncol. 2013;31:344-50.

38. Cairncross G, Wang M, Shaw E, Jenkins R, Brachman D, Buckner J, et al. Phase III Trial of Chemoradiotherapy for Anaplastic Oligodendroglioma: Long-Term Results of RTOG 9402. J Clin Oncol. 2013(3);31:337-43.

39. Boots-Sprenger SHE, Sijben A, Rijntjes J, Tops BBJ, Idema AJ, Rivera AL, et al. Significance of complete 1p/19q co-deletion, IDH1 mutation, and MGMT promoter methylation in gliomas: use with caution. Modern Pathology. 2013;26(7):922-29.

40. IDH2 isocitrate dehydrogenase (NADP(+)) 2 [Homo sapiens (human)].

41. IDH1 isocitrate dehydrogenase (NADP(+)) 1 [Homo sapiens (human)].

42. Lee SH, Jo SH, Lee SM, Koh HJ, Song H, Park JW, et al. Role of NADP+-dependent isocitrate dehydrogenase (NADP+-ICDH) on cellular defence against oxidative injury by gamma-rays. Int J Radiat Biol. 2004;80(9):635-42.

43. Badur MG, Muthusamy T, Parker SJ, Ma S, McBrayer SK, Cordes T. et al. Oncogenic R132 IDH1 Mutations Limit NADPH for De Novo Lipogenesis through (D)2-Hydroxyglutarate Production in Fibrosarcoma Cells. Cell Rep. 2018;25(4):1018-1026. e4.

44. Koh HJ, Lee SM, Son BG, Lee SH, Ryoo ZY, Chang KT, et al. Cytosolic NADP+-dependent Isocitrate Dehydrogenase Plays a Key Role in Lipid Metabolism. J Biol Chem. 2004;279(38):39968-74.

45. Yan H, Parsons DW, Jin G, McLendon R, Rasheed BA, Yuan W, et al. IDH1 and IDH2 Mutations in Gliomas. N Engl J Med. 2009;360:765-73.

46. Nobusawa S, Watanabe T, Kleihues P, Ohgaki H. IDH1 Mutations as Molecular Signature and Predictive Factor of Secondary Glioblastomas. Clin Cancer Res. 2009;15(19):6002-7.

47. Han, S. et al. IDH mutation in glioma: molecular mechanisms and potential therapeutic targets. Br J Cancer. 2020;122(11):1580-89.

48. Choi S, Yu Y, Grimmer MR, Wahl M, Chang SM, Costello JF. Temozolomide-associated hypermutation in gliomas. Neuro Oncol. 2018;20(10):1300-09.

49. Shaw RJ, Kosmatka M, Bardeesy N, Hurley RL, Witters LA, DePinho RA, et al. The tumor suppressor LKB1 kinase directly activates AMP-activated kinase and regulates apoptosis in response to energy stress. Proceedings of the National Academy of Sciences. 2004;101(10):3329-35.

50. PRKAG2 protein kinase AMP-activated non-catalytic subunit gamma 2 [Homo sapiens (human)].

Supplementary Figures

Supp Fig 1

Gene	Annealing temperature	Amplicon size
PRKAA1	60 C	113 bp
PRKAA2	60 C	120 bp
PRKAB1	60 C	137 bp
PRKAB2	58 C/60 C	149 bp
PRKAG1	58 C/60 C	115 bp
PRKAG2	58 C/60 C	194 bp
PRKAG3	58 C	117 bp

Gene	Forward primer sequence	Reverse primer sequence
PRKAA1	TTGAACCTGAAAATGTCCTGCT	GGTGAGCCACAACTTGTTCTT
PRKAA2	CTGCTGGCTTACACAGACCA	GGCGAGGTGAAACTGAAGAC
PRKAB1	CCCTTGCTCAGGGTCCCTTT	CCCTCCGGGGCGTCTTAT
PRKAB2	CCACTGTTATCCGCTGGTCT	GAACTTGTATTGGTGCTCTC
PRKAG1	CAAGAGACCCCAGAATCCAA	CCTGCAGGGACGTATCAAAT
PRKAG2	CGTACCACAACATTGCCTTC	CTGGGTCACCGTGATATCTAG
PRKAG3	GGTGCTGCATCGCTACTACA	ATGGAGACCAGAGGCTTGAA

Supplementary Figure 1: Expression analysis of AMPK subunits in GBM cell lines, normal brain, GBM and LGG patient samples. A) Table showing primer annealing temperatures and amplicon sizes obtained from the primers designed for 7 AMPK genes. B) Table showing forward and reverse primer sequences of the designed primers.

Supp Fig. 2

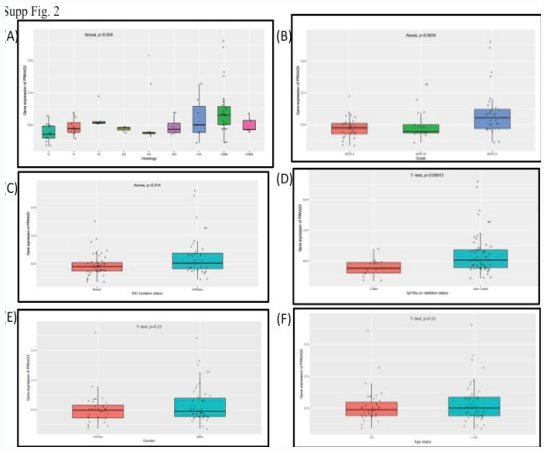

Supplementary Figure 2: In-silico analysis of *PRKAG3* expression across TCGA, HPA, and CCGA datasets. Box plots of mRNA_array_301 dataset in CGGA showing expression of *PRKAG3* in different categories (a) Histology (b) grade (c) IDH mutation (d)1p/19q deletion status (e) gender (f) age status.

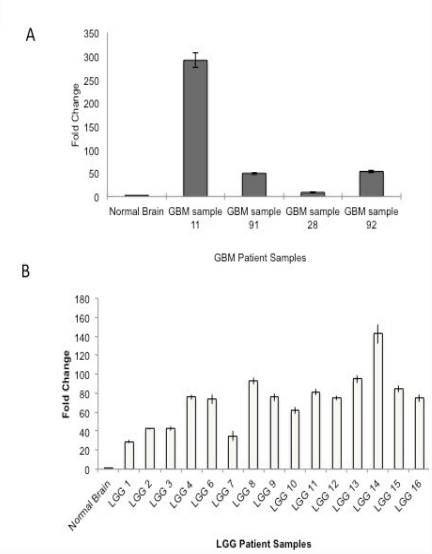

Supplementary Figure 3: Identification of novel isoforms of *PRKAG3* in GBM and LGG samples. (A) Bar graph depicting fold change expression of *PRKAG3* as obtained through RTPCR in 2 male and 2 female GBM samples with respect to normal brain. (B) Bar graph depicting relative amplicon intensity of *PRKAG3* bands in LGG Patients. Mean gray values obtained through Image J.

A

Primer	FP (5'-3')	RP (5'-3')	Amplicon size
PRKAG3 I	GGGCTGGAGCACGCACTGCGCA	CCGACTTCTGCCTTGTCCAT	187 bp
PRKAG3 II	CACATTCCCCAAGACCACAC	CAGGCCTTCTAGCTCACACT	184 bp
PRKAG3 III	TCTACCTGCAAGGCTGCTTC	TGTGGAGTACGTTGCCTGAC	138 bp
PRKAG3 IV	ATTCCGAGACTTGGCTGTGG	CACCAGTGCCTGAAGGATGT	370 bp

Supplementary Figure 4: Scanning of other exon junctions of one GBM patient cDNA. A) Table showing primer sequences of the newly designed *PRKAG3* primers along with their amplicon size. B) Gel image of the PCR products obtained upon amplifying GBM patient sample no. 7 using the 4 new primer pairs.

Supp Fig 5

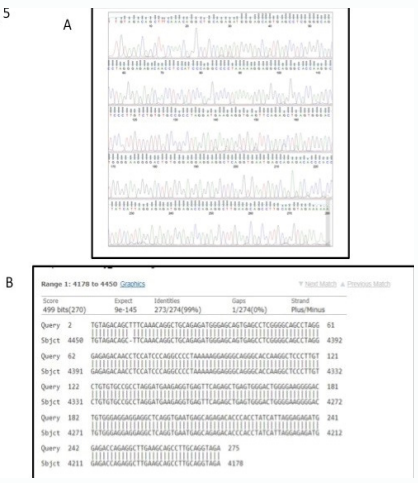

Supplementary Figure 5: Intron retention revealed from sequencing of novel isoforms. A) Sequencing results in the form of electropherograms for PCR product obtained by amplifying GBM patient sample no. 7 using the newly designed primer pair *PRKAG3*-III. B) BLAST of obtained sequence of sample 7 amplicon against the CDS of *PRKAG3*.